IEEE Photonics Journal
An IEEE Photonics Society Publication

Investigation on the Stability of WSe_2-PVA Saturable Absorber in an all PM Q-Switched Fiber Laser

Volume 8, Number 5, October 2016

Chaoshi Guo
Bohua Chen
Hao Wang
Xiaoyan Zhang
Jun Wang
Kan Wu
Jianping Chen

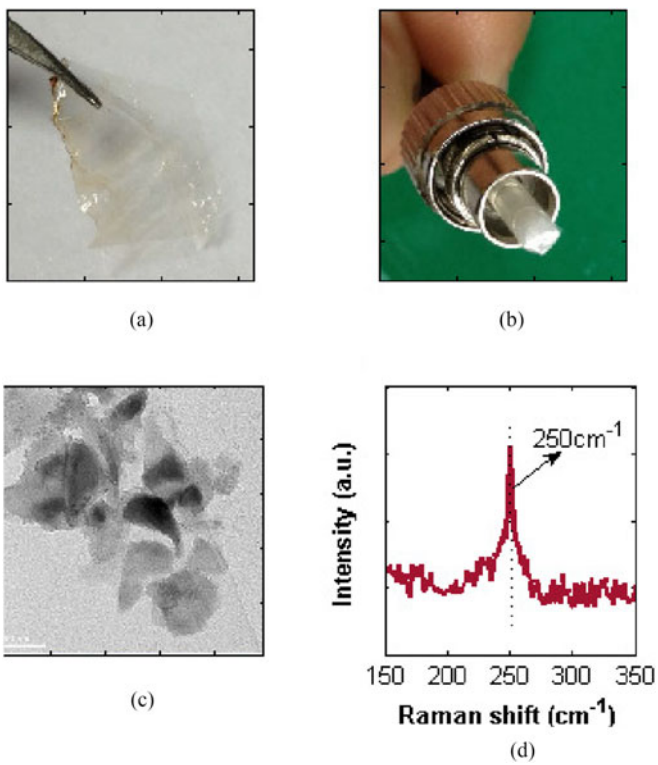

DOI: 10.1109/JPHOT.2016.2603223
1943-0655 © 2016 IEEE

Investigation on the Stability of WSe_2-PVA Saturable Absorber in an all PM Q-Switched Fiber Laser

Chaoshi Guo,[1] Bohua Chen,[1] Hao Wang,[1] Xiaoyan Zhang,[2] Jun Wang,[2] Kan Wu,[1] and Jianping Chen[1]

[1]State Key Laboratory of Advanced Optical Communication Systems and Networks, Department of Electronic Engineering, Shanghai Jiao Tong University, Shanghai 200240, China.
[2]Key Laboratory of Materials for High-power Laser, Shanghai Institute of Optics and Fine Mechanics, Chinese Academy of Sciences, Shanghai 201800, China.

DOI:10.1109/JPHOT.2016.2603223

Manuscript received July 14, 2016; revised August 21, 2016; accepted August 22, 2016. Date of current version September 14, 2016. This work was supported in part by the Shanghai Yangfan Program under Grant 14YF1401600; in part by the NSFC under Grant 61505105, Grant 51302285, and Grant 61522510; in part by the External Cooperation Program of BIC; the Chinese Academy of Sciences (CAS) under Grant 181231KYSB20130007; in part by the Fundamental Research Funds for the Central Universities under Grant 2232014D3-28; and in part by the "Strategic Priority Research Program" of CAS under Grant XDB160307. Corresponding authors: K. Wu (e-mail: kanwu@sjtu.edu.cn).

Abstract: In this paper, we demonstrate an all polarization maintaining (PM) Q-switched erbium-doped fiber laser based on tungsten diselenide-polyvinyl alcohol (WSe_2−PVA) saturable absorber (SA) and investigated the stability of WSe_2−PVA SA in the laser. The all PM cavity isolated the environmental perturbation on the cavity birefringence so that the evolution of material properties of WSe_2−PVA SA during the Q-switched operation can be investigated based on the laser output. It is found that when heat accumulation reached a certain level in WSe_2−PVA SA, PVA in SA would first melt and perturb the transmission of SA; then, WSe_2 in SA would be quickly damaged, resulting in a permanent increase of the SA loss. This work will benefit the research on obtaining a long-term stable all PM Q-switched lasers based on 2-D material saturable absorber.

Index Terms: Q-switched lasers, erbium lasers, fiber lasers.

1. Introduction

Graphene, the best-known 2-D nano-material, which owns excellent optoelectronic characteristics, has attracted increasing interest in researching on 2-D materials since the emergence of it in 2004 [1]–[9]. In recent years, another kind of 2-D material called transition metal dichalcogenides (TMDs), which show analogous physical properties compared to graphene, have become a popular research hotspot [10]–[20]. At the same time, various optical and electrical characteristics such as saturable absorption, four wave mixing and wavelength conversion have been reported [21]–[26]. Among these promising properties, wideband absorption spectrum and saturable absorption act as the key roles in some important photonic applications such as mode-locked lasers [7], [27]–[29] and Q-switched lasers [30]–[34]. As summarized in [35], TMDs have a generalized formula of MX_2, where M represents transition metal atom such as Mo and W, and X represents chalcogenide atom such

as S and Se. Recently, numerous researchers have investigated the applications of these TMDs as saturable absorbers (SAs) in Q-switched fiber lasers or mode-locked fiber lasers. In 2014 R.I. Woodward used the molybdenum disulfide (MoS_2) as the saturable absorber to realize a tunable Q-switched fiber laser [34]. In 2015, Wu utilized the WS_2 as saturable absorber to realize a stable mode-locked fiber laser [36] while in the same year, Chen compared the performance difference of four materials (WSe_2, WS_2, $MoSe_2$, and MoS_2) in a Q-switched fiber laser [37]. It can be seen that TMDs have played an important role in the field of fiber lasers. Meanwhile, polarization maintaining (PM) cavity has been widely used in various laser designs for its stable birefringence property. Nishizawa used carbon nanotube as saturable absorber and realized an all PM fiber laser in 2010 [38]. Sobon reported an all PM mode-locked fiber laser by graphene saturable absorber in 2012 [39]. Zhao used an all PM cavity to study passively mode-locked fiber laser based the semiconductor saturable absorber mirror in 2013 [40]. Although many mode-locked or Q-switched lasers with PM cavities have been reported, it is still unclear how the TMDs based saturable absorbers perform in an all PM laser cavity. Moreover, a systematic study on the stability of the TMD SAs under laser operation has not been reported yet. Therefore, it is meaningful to investigate how the property of a TMD SA evolves during the laser operation and affects the output of the laser, which may benefit the future research on TMD SAs to obtain a long-term stable high-performance laser.

In this paper, we investigated the stability of the prepared WSe_2-polyvinyl alcohol (PVA) SA in an all PM Q-switched fiber laser. The all PM cavity isolated the environmental influence on the cavity birefringence, which enabled us to investigate the stability of the WSe_2-PVA SA during Q-switched operation. It is observed that the prepared WSe_2-PVA SA can sustain a stable Q-switched operation during an observation time of -1.6 hours under medium pump power of 280 mW, but would be gradually damaged if the pump power exceeded 300 mW due to the thermal accumulation. The laser performance before and after the damage of WSe_2-PVA SA was compared and the process of the physical damage of the SA was discussed. It is believed that this work will benefit the research of obtaining a long-term stable all PM Q-switched fiber lasers, as well as a stable material based saturable absorber.

2. Material Preparation and Characterization

Saturable absorber is a key component for Q-switched or mode-locked lasers. Here, we introduce the preparation and characterization of WSe_2-PVA SA. Briefly, 5 mg/ml WSe_2-PVA water dispersions with sodium cholate as surfactant were prepared using the liquid-phase exfoliation (LPE) method. Ultra-sonication and centrifugation processing were utilized to obtain WSe_2 nanosheets with few layers and small size. Meanwhile 50 mg/ml polyvinyl alcohol (PVA) aqueous solution was also prepared. Then, 2 ml WSe_2-PVA dispersions and 10 ml PVA solution were mixed for 24 hours by a magnetic stirrer. The mixture was processed by ultrasonic water bath device for another 4 hours for a thorough mixing. Finally, WSe_2-PVA mixture was transferred to the surface of a clean dish and dried under 50 °C condition for 3 days to obtain WSe_2-PVA thin film. More details can be referred to [37]. Fig. 1 shows some properties of the material. Fig. 1(a) shows a prepared WSe_2-PVA thin film. WSe_2-PVA thin film was further cut into small pieces of -1 mm $\times$ 1 mm and transferred onto a fiber end to function as a SA, as shown in Fig. 1(b). Fig. 1(c) shows the transmission electron microscopy photo of WSe_2 nanosheets. The size of the nanosheets is -200×250 nm. Atomic force microscope measurement indicated that the number of layers of nanosheets is from 2–6. Also, LPE method can produce large quantity of nanosheets but cannot precisely control the size and thickness of the nanosheets. Fig. 1(d) shows the Raman spectrum of WSe_2-PVA. The peak near 250cm^{-1} corresponded to the out-of-plane motion of WSe_2 molecular [41].

The nonlinear transmission is an important parameter for the prepared WSe_2-PVA saturable absorber. A standard two-arm nonlinear transmission experiment was carried out, shown in Fig. 2. A mode-locked laser generated pulse train with a repetition rate of 37 MHz and pulse width of 560 fs. The light from the mode-locked laser propagated through an isolator that protected the laser and entered into a 99:1 coupler (denoted as coupler 1). One-percent output of the coupler went into an optical power meter (power meter 1) as a reference, and 99% output went through

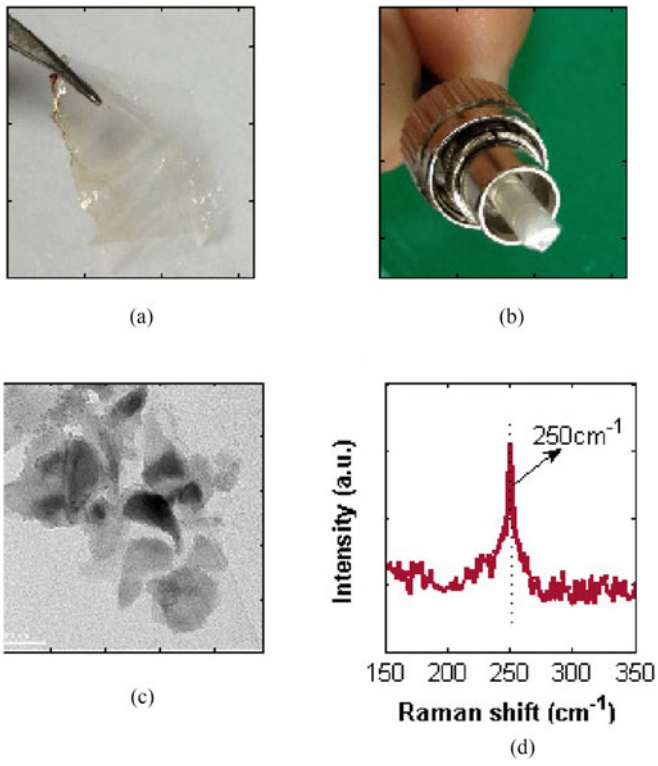

Fig. 1 (a) WSe_2−PVA thin film. (b) WSe_2−PVA transferred onto the surface of a fiber connector as SA. (c) Transmission electron microscopy image of WSe_2. (d) Raman spectrum of WSe_2−PVA thin film.

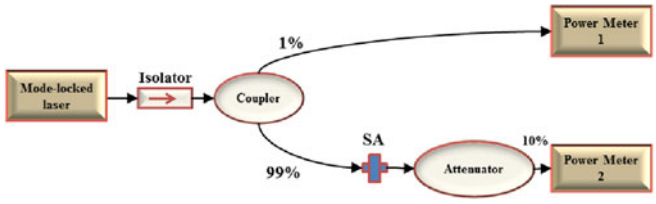

Fig. 2. Experiment setup of the nonlinear transmission of WSe_2−PVA SA.

the WSe_2−PVA SA and into another optical power meter (power meter 2) for the measurement. A 10 dB attenuator was inserted before power meter 2 to meet the power requirement of the power meter. The WSe_2−PVA SA was sandwiched between two FC/PC fiber connectors.

By tuning the output power of the mode-locked laser, nonlinear transmission of the WSe_2−PVA SA was obtained, shown in Fig. 3. The following formula of saturable absorption was used to fit the experiment data [42]:

$$T(I) = 1 - \Delta T(\exp)(-I/I_{sat}) - T_{ns} \quad (1)$$

where ΔT is modulation depth, I is optical intensity, I_{sat} is saturation intensity, and the T_{ns} is non-saturable absorbance. The fluctuation between the experimental data and the fitting curve were mainly caused by the environmental perturbation and the uncertainty of the power meters. For the WSe_2−PVA SA sample under test, the modulation depth is 4.31%, the saturation intensity is 7.97 MW/cm^2, and the non-saturable absorbance T_{ns} is 56.8%.

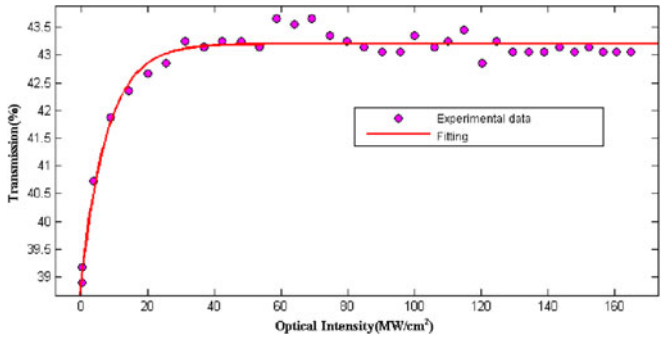

Fig. 3. Saturable absorption property of WSe_2–PVA SA.

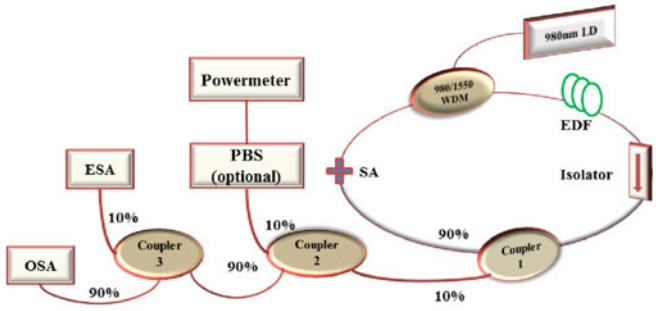

Fig. 4. Schematic design of the PM Q-switched erbium-doped fiber laser.

3. Experiments and Results

3.1 All Polarization Maintaining Fiber Laser

To investigate the stability of WSe_2–PVA SA during the Q-switched operation, the output properties of the Q-switched laser would be an important reference. Thus, a laser cavity which is insensitive to the environmental perturbation would be desired, i.e., an all PM cavity would be necessary for the experiment. In this section, an all PM Q-switched fiber laser based on WSe_2–PVA SA was made and characterized.

The experimental setup of the all PM Q-switched laser is showed in Fig. 4. A 980 nm laser diode (LD) provided the pump power for the laser operation. A wavelength division multiplexer (WDM) coupled the 980 nm light into the ring cavity. Erbium-doped fiber (EDF) was used as the gain medium. WSe_2–PVA SA was incorporated in the cavity by being sandwiched between a pair of FC/PC connectors. A 90:10 fiber coupler extracted 10% of the intra-cavity power for the output. The output power was further split by two fiber couplers for the measurement of optical spectrum (YOKOGAWA AQ6370C), electrical spectrum (ROHDE&SCHWARZ FSUP), and optical power meter. All the components in the cavity were polarization maintaining, which isolated the environmental perturbation on the birefringence of the cavity and sustained a stable linear polarization state all the time. With this all PM structure, the long-term stability of the prepared WSe_2–PVA SA can be investigated. The stability property of the WSe_2–PVA SA will be investigated in Section 3.2. The polarization beam splitter (PBS) before the power meter was also used for the investigation of SA stability in Section 3.2. In this section the general output properties of the laser were provided.

When pump power was 20 mW, the laser operated in a continuous wave state indicating the low loss in the cavity. When the pump power reached 130 mW, Q-switched operation was built up but still unstable. A stable Q-switched operation with low amplitude fluctuation was obtained when the pump power was further increased to 170 mW. Under the pump power ranging from 170 mW to

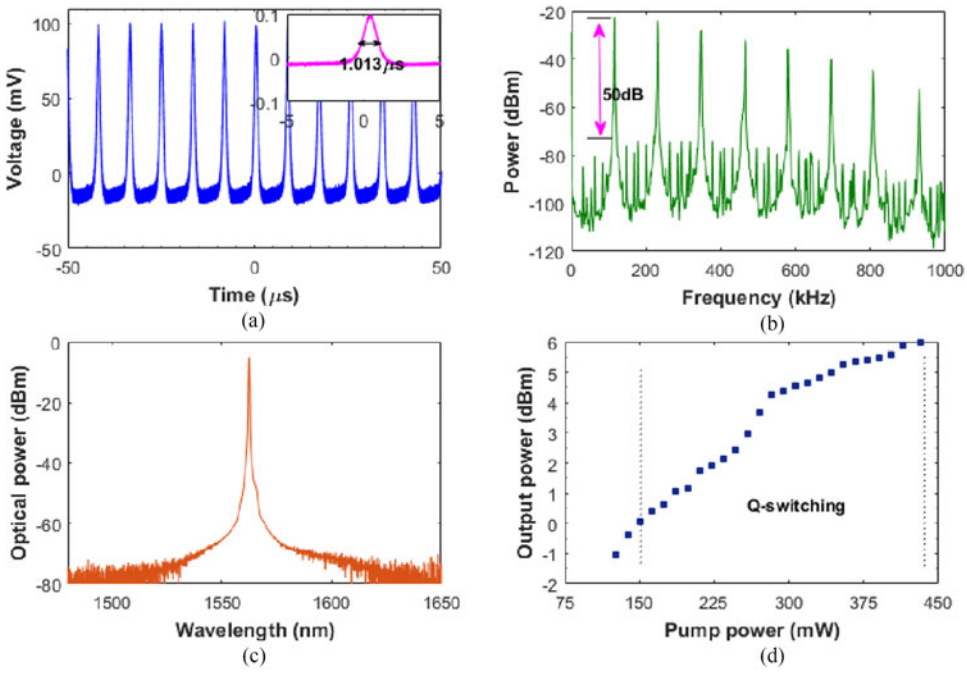

Fig. 5. (a) Oscilloscope trace under 280 mW pump power of PM fiber laser, (b) electrical spectrum, (c) optical spectrum, and (d) output power with respect to pump power.

300 mW, a stable Q-switched operation can be obtained. For the pump power from 300 mW to 430 mW, Q-switched operation still existed but became less stable which was considered to be caused by the material property change of the prepared WSe_2-PVA SA under high intra-cavity power. More details of the investigation on the property evolution of SA will be provided in Section 3.2.

Fig. 5 summarizes the output properties of the Q-switched state of the laser. Fig. 5(a) shows a typical pulse train waveform in the time domain under a pump power of 280 mW. The pulse width shown in the inserted was 1.013 μs. The output power was 4.25 dBm and the repetition rate was 112.23 kHz, corresponding to a pulse energy of -23 nJ. Fig. 5(b) shows the electrical spectrum measured by an electrical spectrum analyzer with a span of 1 MHz. The extinction ratio was -50 dB showing the good stability of the laser operation. Fig. 5(c) shows the optical spectrum with a center wavelength of 1560 nm, which showed the low loss property of the cavity and Fig. 5(d) shows the relation between the output power and the injected pump power. For the power ranging from 300 mW to 430 mW, the measurement was conducted within a short time because operation for a long duration under such a high pump power level would damage WSe_2-PVA SA as discussed in Section 3.2. On the other hand this less stable operation region provided an opportunity to investigate how the property of the SA degraded from a normal status to a damaged status.

Pulse duration and repetition rate are another two important parameters for the Q-switched fiber laser. These two parameters were measured by the oscilloscope, shown in Fig. 6(a). For the pump power from 130 mW to 170 mW, the Q-switched operation was not very stable and the pulse amplitude varied from time to time. When the pump power was above 170 mW, a stable Q-switched state with constant pulse amplitude was obtained. So we can see the variation of these two parameters in the Fig. 6(a), with the increase of the pump power from 170 mW to 430 mW, the repetition frequency increased from 92.46 kHz to 138 kHz while the pulse duration decreased from 1.478 μs to 0.754 μs. These trends were consistent with the reported evolution of the Q-switched operation when the pump power was increased. The corresponding pulse energy varied from -12 nJ to -29 nJ, as shown in Fig. 6(b).

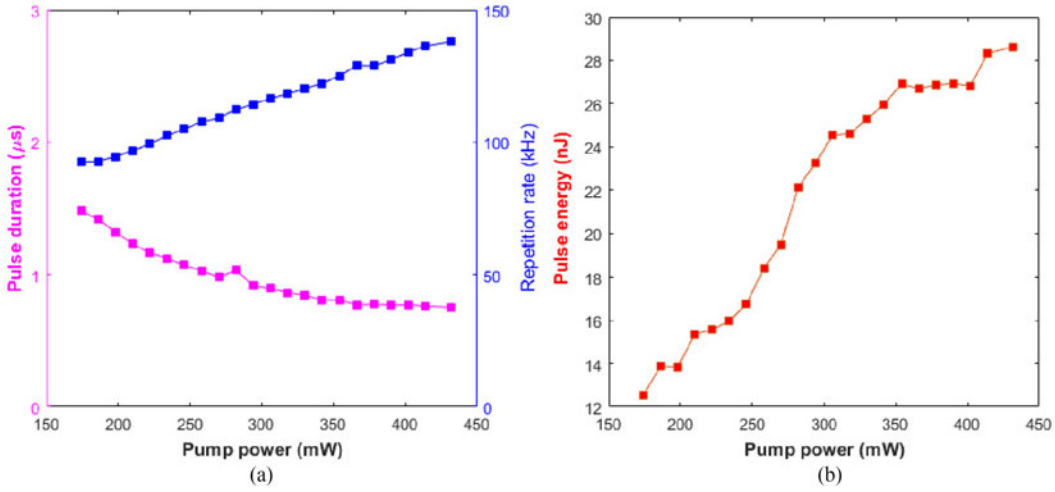

Fig. 6. (a) Repetition frequency and pulse duration with respect to pump power and (b) pulse energy with respect to pump power.

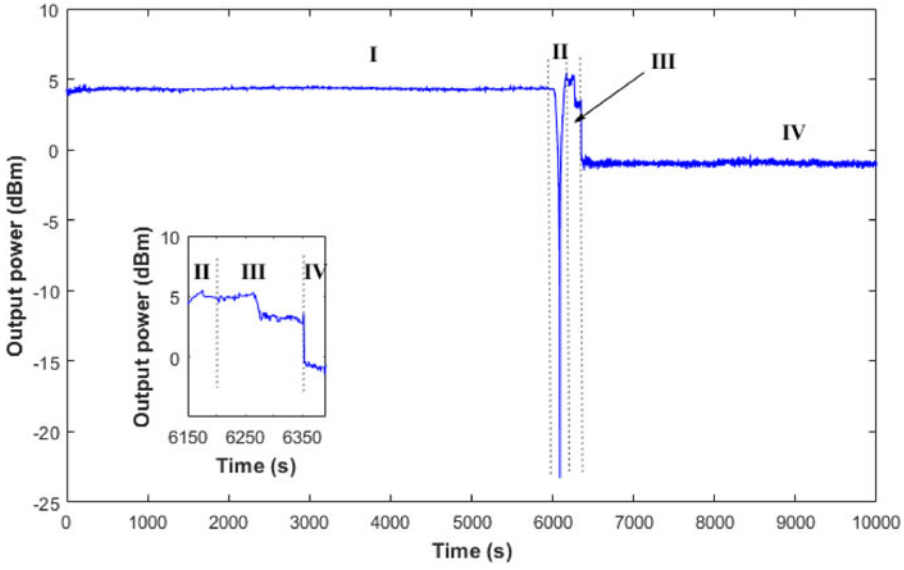

Fig. 7. Variation of the laser output power in a period of −10 000 seconds.

3.2 Investigation on the Stability of WSe_2−PVA *SA*

In this section, the stability of the prepared WSe_2−PVA SA was investigated. The purpose was to evaluate the property evolution of WSe_2−PVA SA during the Q-switched operation. Therefore the output of the Q-switched laser became a very important real-time reference. The choice of an all PM cavity helped to isolate the influence on the cavity birefringence caused by the environmental perturbation.

The laser was operated continuously for 3 hours. During this period, the output optical power was recorded automatically by a computer controlled optical power meter every 1 second, shown in Fig. 7. There were four regions representing different operation states of the laser. In region I, the laser operated in a stable Q-switched state for 6000 s (−1.6 hours). The pump power was fixed to 280 mW. The output power was 4.25 dBm and pulse energy was −23 nJ. It can be observed that

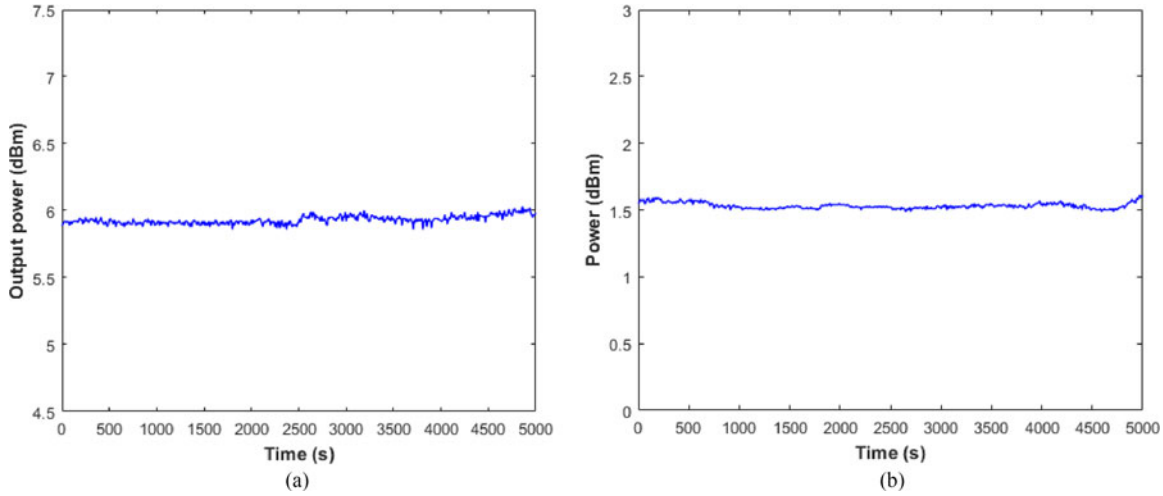

Fig. 8. (a) Variation of the laser output power without SA in the cavity. (b) Variation of the laser output power after a PBS indicating the polarization stability of the laser.

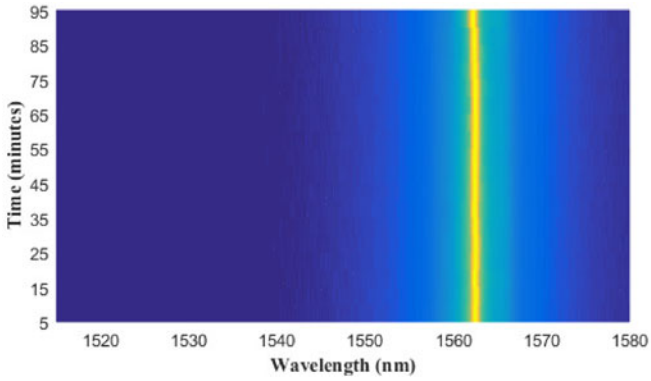

Fig. 9. Optical spectra of the laser during a stable Q-switched operation.

the output was stable with a fluctuation less than 0.25 dB. For comparison, the output power from a laser cavity without SA was also recorded, shown in Fig. 8(a). Such a laser operated in continuous wave state. The variation of the output power was −0.1 dB. Because the output variation was 0.25 dB for the Q-switched laser, it meant the SA contributed −0.15 dB fluctuation. Although the SA was not damaged under the pump power of 280 mW, this additional power fluctuation indicated that heat had still gradually accumulated during the laser operation and the property of SA had been slightly changed. We also investigated the stability of the output polarization state. A polarization beam splitter was inserted before the power meter shown in Fig. 4. The output of one arm of the PBS was monitored by the power meter for a duration of 5000 s, shown in Fig. 8(b). The variation was also less than 0.25 dB. The optical spectra and electrical spectra of the Q-switched laser were recorded with an interval of 5 minutes during this period, shown in Figs. 9 and 10, respectively. In Figs. 9 and 10, the horizontal axis represents the frequency and the vertical axis represents the time. Brighter color represents higher power of the spectrum. It can be observed that the center wavelength in the optical spectra was nearly unchanged, showing a good stability of the laser and the material. The electrical frequency spectrum had some variation which was considered to be caused by the temperature change. These results suggested that the prepared WSe_2−PVA SA can sustain a stable material property and thus a stable Q-switched operation under a pump power

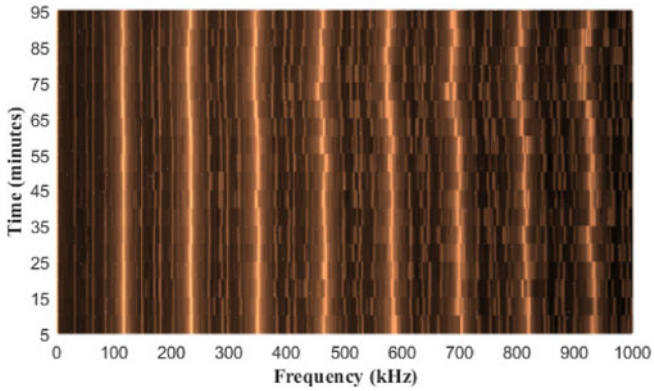

Fig. 10. Electrical spectra of the laser during a stable Q-switched operation.

of 280 mW for a duration of ~1.6 hours. The corresponding output power was 4.25 dBm, and the pulse energy was ~23 nJ.

Then, the pump was deliberately decreased and increased to see how the SA reacted to the condition change in the cavity, denoted as region II in Fig. 7. The maximum pump power was increased to 430 mW corresponding to an output power of 5.49 dBm. This power was lower than that of 5.95 dBm shown in Fig. 5(d) measured at the same pump power because the data in Fig. 5(d) was measured at the beginning of the laser operation while data here was measured after the continuous operation of 1.6 hours. This phenomenon again indicated that the heat, although did not damage the SA, had slowly accumulated in the SA during the Q-switched operation, and when the pump power increased to a higher level, the heat accumulation reached a certain level and began to affect the property of the SA. One can also note that when the pump power was increased from 280 mW to 430 mW, the pulse energy was just slightly increased from 23 nJ to 25.6 nJ (0.45 dB increase) while the output power was significantly increased from 4.25 dBm to 5.49 dBm (1.24 dB increase), therefore it was the average power rather than the pulse energy that led to the property change of the SA. With this heat accumulation, PVA in the SA had begun to melt. At the end of region II, the pump power was turned back to 280 mW. However, PVA of WSe_2–PVA SA had been partially melted and led to an unstable transmission of the SA. As a result, the laser output power became less stable as shown in region III in Fig. 7. The variation of the output power increased to ~2 dB. This unstable state existed in a duration of ~150 s. Because the SA was sandwiched between two connectors, this property change of the SA perturbed the light propagation between two connectors and led to the quick heat accumulation in the SA. When the heat accumulation reached an even higher threshold, the WSe_2 nanosheets in the SA began to be damaged and the transmission of the SA suddenly dropped. Accordingly, the laser output also dropped quickly to a low level within a very short time, denoted as region IV in Fig. 7. Clear details were shown in the inset of Fig. 7. The transition from region III to region IV happened only in a few seconds. The damage led to a permanent change of the SA property. In region IV, the lower average power induced less heat and another heat balance was reached in the SA. The output power became stable but higher fluctuation can be clearly observed compared with region I.

The oscilloscope traces, electrical spectra and optical spectra before (see Fig. 11(a)–(c)) and after (see Fig. 11(d)–(f)) the damage of SA are summarized in Fig. 11. It can be clearly observed that the pulse amplitude had significantly reduced from ~100 mV to ~25 mV after the photodetector when the SA was damaged. The electrical spectrum also dropped to a low power level after the damage of SA. The envelope of the frequency peaks was determined by the Fourier transform of the time-domain waveform and therefore decreased with the increase of frequency. The change of optical spectrum was even more obvious. The center wavelength had moved from 1560 nm to 1530 nm, which indicated that the cavity loss had drastically increased.

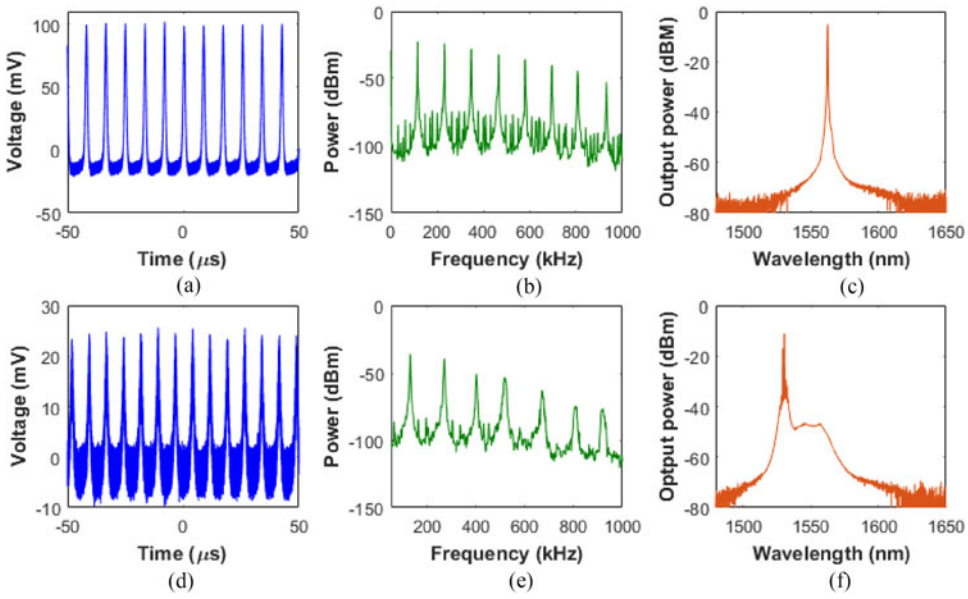

Fig. 11. (a) Oscilloscope waveform, (b) electrical spectrum, and (c) optical spectrum of the fiber laser when the WSe_2−PVA SA was undamaged. (d) Oscilloscope waveform, (e) electrical spectrum, and (f) optical spectrum of the fiber laser when the WSe_2 -PVA SA was damaged.

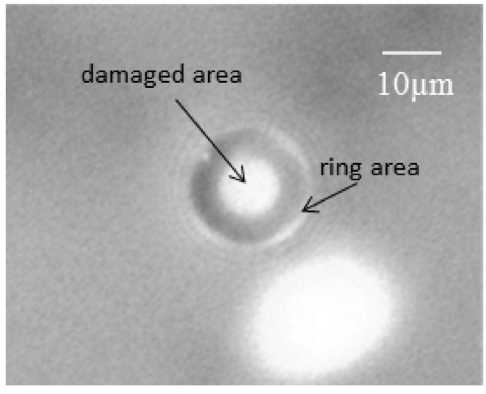

Fig. 12. Microscopic image of the damaged WSe_2−PVA SA.

To further verify the damage of the SA, a microscopic image of the SA was taken, which is shown in Fig. 12. In the middle of Fig. 12, a round damage area can be clearly observed. Outside the damaged area there was a ring area. This was caused by the pressure between two convex and curved end surfaces of the connectors, especially when the PVA was melted by the high optical power.

4. Discussion

To demonstrate the stability of the PM Q-switched fiber laser, a non-PM Q-switched fiber laser was built for comparison. The experimental setup is shown in Fig. 13. The general design was very similar to the all PM cavity shown in Fig. 4. The difference was that all the components were non-PM and there was a polarization controller (PC) in the cavity to adjust the cavity birefringence. The SA was still WSe_2−PVA. Typical output properties of such a non-PM Q-switched laser are summarized in Fig. 14. Fig. 14(a) shows a typical pulse train waveform in the time domain under a pump power

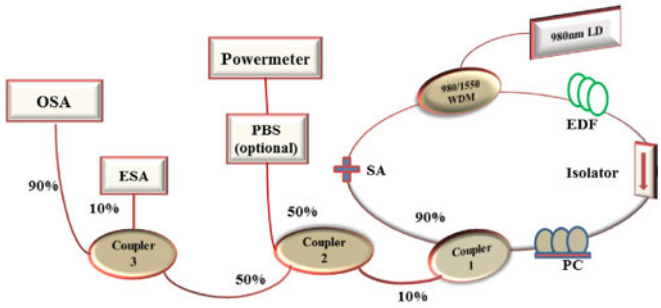

Fig. 13. Schematic design of the Non-PM erbium-doped fiber laser.

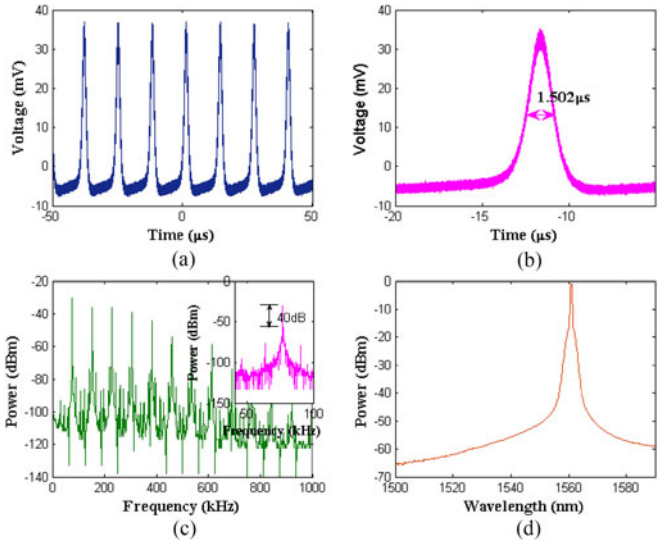

Fig. 14. (a) Oscilloscope trace under 310 mW pump power of Non-PM fiber laser, (b) single pulse profile spectrum, (c) frequency spectrum (inset shows a 40 dB extinction rate at fundamental frequency), and (d) optical spectrum.

of 310 mW. The pulse width shown in Fig. 14(b) was 1.502 μs. The output power was 1.5 dBm and the repetition frequency was 77.286 kHz, corresponding to a single pulse energy of -18 nJ. Fig. 14(c) shows the electrical spectrum measured by an electrical spectrum analyzer with a span of 1 MHz. The extinction ratio was -40 dB showed in the inset. Fig. 14(d) shows the optical spectrum. The center wavelength was near 1560 nm which indicated the low cavity loss of the laser.

To show the difference of the stability between the PM laser and non-PM laser, we investigated the stability of the output polarization state. A PBS was inserted before the power meter and the output power from the PBS was recorded in a time period of 5000 s. The measurement result is shown in Fig. 15(a). The power fluctuation was -0.5 dB which was higher than that of the all PM laser. The output power evolution from the non-PM Q-switched laser was measured for another 5000 s, shown in Fig. 15(b). It can be clearly observed that the power had varied seriously compared with the output from the all PM laser, which suggested that the polarization state of the non-PM laser had changed from time to time. This result indicated the non-PM laser was more vulnerable to the environment perturbation compared with the all PM laser. Therefore, an all PM laser provided a more stable platform for the investigation on the material property of the SA.

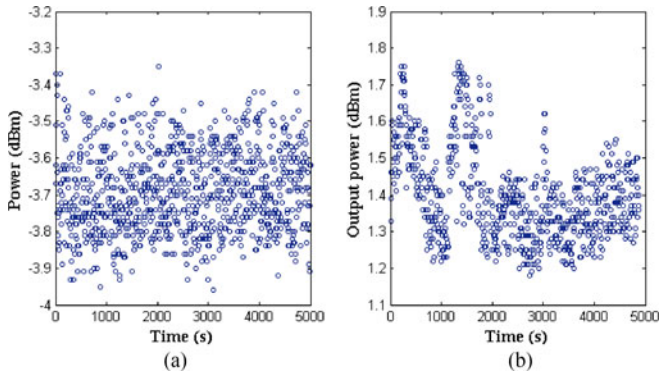

Fig. 15. (a) Power from the PBS under 310 mW pump power of Non-PM fiber laser. (b) Output power under 310 mW pump power of non-PM fiber laser.

5. Conclusion

In conclusion, this paper investigated the stability of WSe_2–PVA saturable absorber in an all polarization maintaining erbium-doped fiber laser under Q-switched operation. The all PM cavity isolated the influence of the environment and sustained only one polarization state in the cavity, which enabled us to focus on the stability of the material. From the results of the stability experiment, it was found the prepared WSe_2–PVA SA can work stably for 1.6 hours during Q-switched operation under pump power of 280 mW but would be gradually damaged if the pump power increased to 430 mW due to the thermal accumulation. The detailed process for how a WSe_2–PVA SA degraded from a normal status to a damaged status has been clearly revealed. It is believed that this work will benefit research on obtaining a long-term stable material based saturable absorber.

References

[1] F. Bonaccorso, Z. Sun, T. Hasan, and A. C. Ferrari, "Graphene photonics and optoelectronics," *Nature Photon.*, vol. 4, pp. 611–622, 2010.
[2] K. K. Chow, M. Tsuji, and S. Yamashita, "Single-walled carbon-nanotube-deposited tapered fiber for four-wave mixing based wavelength conversion," *Appl. Phys. Lett.*, vol. 96, 2010, Art. no. 061104.
[3] Y. Feng *et al.*, "Saturable absorption behavior of free-standing graphene polymer composite films over broad wavelength and time ranges," *Opt. Exp.*, vol. 23, pp. 559–569, 2015.
[4] Q. Hao, Z. Guo, Y. Liu, W. Li, Q. Zhang, and H. Zeng, "Spectrally tailored supercontinuum generation from single-mode-fiber amplifiers," *Appl. Phys. Lett.*, vol. 104, 2014, Art. no. 201112.
[5] K. Kashiwagi, S. Yamashita, and S. Y. Set, "In-situ monitoring of optical deposition of carbon nanotubes onto fiber end," *Opt Exp.*, vol. 17, pp. 5711–5715, Mar. 30, 2009.
[6] M. Liu *et al.*, "A graphene-based broadband optical modulator," *Nature*, vol. 474, pp. 64–67, Jun. 2011.
[7] M. Liu *et al.*, "Microfiber-based few-layer MoS2 saturable absorber for 2.5 GHz passively harmonic mode-locked fiber laser," *Opt. Exp.*, vol. 22, pp. 22841–22846, Sep. 22, 2014.
[8] A. Martinez, K. Fuse, B. Xu, and S. Yamashita, "Optical deposition of graphene and carbon nanotubes in a fiber ferrule for passive mode-locked lasing," *Opt. Exp.*, vol. 18, pp. 23054–23061, Oct. 22, 2010.
[9] N. Papasimakis *et al.*, "Graphene in a photonic metamaterial," *Opt. Exp.*, vol. 18, pp. 8353–8359, Apr. 12, 2010.
[10] D. Mao *et al.*, "Flexible high-repetition-rate ultrafast fiber laser," *Sci. Rep.*, vol. 3, 2013, Art. no. 3223.
[11] D. Mao *et al.*, "WS2 mode-locked ultrafast fiber laser," *Sci. Rep.*, vol. 5, 2015, Art. no. 7965.
[12] K. Wang *et al.*, "Ultrafast saturable absorption of two-dimensional MoS2 nanosheets," *ACS Nano*, vol. 7, pp. 9260–9267, Oct. 22, 2013.
[13] R. I. Woodward *et al.*, "Few-layer MoS2 saturable absorbers for short-pulse laser technology: Current status and future perspectives [Invited]," *Photon. Res.*, vol. 3, pp. A30–A42, Apr. 1, 2015.
[14] P. Yan *et al.*, "Q-switched fiber laser using a fiber-tip-integrated TI saturable absorption mirror," *IEEE Photon. J.*, vol. 8, no. 1, pp. 1–6, Feb. 2016.
[15] P. Yan *et al.*, "Microfiber-based WS2-film saturable absorber for ultra-fast photonics," *Opt. Mater. Exp.*, vol. 5, pp. 479–489, Mar. 1, 2015.
[16] X. Zhang *et al.*, "Facile fabrication of wafer-scale MoS2 neat films with enhanced third-order nonlinear optical performance," *Nanoscale*, vol. 7, pp. 2978–2986, 2015.
[17] T. Carrig, "Transition-metal-doped chalcogenide lasers," *J. Electron. Mater.*, vol. 31, pp. 759–769, Jul. 1, 2002.

[18] Y.-H. Lee *et al.*, "Synthesis of large-area MoS2 atomic layers with chemical vapor deposition," *Adv. Mater.*, vol. 24, pp. 2320–2325, 2012.
[19] R. S. Mane and C. D. Lokhande, "Chemical deposition method for metal chalcogenide thin films," *Mater. Chem. Phys.*, vol. 65, pp. 1–31, Jun. 15, 2000.
[20] H. Wang *et al.*, "Ethanol catalytic deposition of MoS2 on tapered fiber," *Photon. Res.*, vol. 3, pp. A102–A107, Jun. 1, 2015.
[21] R. Khazaeinezhad, S. Hosseinzadeh Kassani, H. Jeong, D.-I. Yeom, and K. Oh, "Femtosecond soliton pulse generation using evanescent field interaction through tungsten disulfide (WS2) film," *J. Lightw. Tech*, vol. 33, no. 17, pp. 3550–3557, Sep. 1, 2015.
[22] A.-P. Luo, M. Liu, X.-D. Wang, Q.-Y. Ning, W.-C. Xu, and Z.-C. Luo, "Few-layer MoS2-deposited microfiber as highly nonlinear photonic device for pulse shaping in a fiber laser [Invited]," *Photon. Res.*, vol. 3, pp. A69–A78, Apr. 1, 2015.
[23] D. Mao, X. Liu, D. Han, and H. Lu, "Compact all-fiber laser delivering conventional and dissipative solitons," *Opt. Lett.*, vol. 38, pp. 3190–3193, Aug. 15, 2013.
[24] D. Mao, X. Liu, and H. Lu, "Observation of pulse trapping in a near-zero dispersion regime," *Opt. Lett.*, vol. 37, pp. 2619–2621, Jul. 1, 2012.
[25] R. I. Woodward *et al.*, "Wideband saturable absorption in few-layer molybdenum diselenide (MoSe2) for Q-switching Yb-, Er- and Tm-doped fiber lasers," *Opt. Exp.*, vol. 23, pp. 20051–20061, Jul. 27, 2015.
[26] V. Y. Fominskii, S. N. Grigor'ev, R. I. Romanov, and V. N. Nevolin, "Effect of the pulsed laser deposition conditions on the tribological properties of thin-film nanostructured coatings based on molybdenum diselenide and carbon," *Tech. Phys.*, vol. 57, pp. 516–523, Apr. 1, 2012.
[27] S. S. Huang *et al.*, "Soliton rains in a graphene-oxide passively mode-locked ytterbium-doped fiber laser with all-normal dispersion," *Laser Phys. Lett.*, vol. 11, 2014, Art. no. 025102.
[28] I.-G. Lee *et al.*, "Unidirectional emission from a cardioid-shaped microcavity laser," *Opt. Exp.*, vol. 24, pp. 2253–2258, Feb. 8, 2016.
[29] H. Liu *et al.*, "Femtosecond pulse erbium-doped fiber laser by a few-layer MoS2 saturable absorber," *Opt. Lett.*, vol. 39, pp. 4591–4594, Aug. 1, 2014.
[30] H. Ahmad *et al.*, "Passively Q-switched erbium-doped fiber laser at C-band region based on WS2 saturable absorber," *Appl. Opt.* vol. 55, pp. 1001–1005, Feb. 10, 2016.
[31] Y. Huang *et al.*, "Widely-tunable, passively Q-switched erbium-doped fiber laser with few-layer MoS2 saturable absorber," *Opt. Exp.*, vol. 22, pp. 25258–25266, Oct. 20, 2014.
[32] S. H. Kassani, R. Khazaeinezhad, H. Jeong, T. Nazari, D.-I. Yeom, and K. Oh, "All-fiber Er-doped Q-Switched laser based on Tungsten Disulfide saturable absorber," *Opt. Mater. Exp.*, vol. 5, pp. 373–379, Feb. 1, 2015.
[33] Z. Luo *et al.*, "1.06 μm Q-switched ytterbium-doped fiber laser using few-layer topological insulator Bi2Se3 as a saturable absorber," *Opt. Exp.*, vol. 21, pp. 29516–29522, Dec. 2, 2013.
[34] R. I. Woodward *et al.*, "Tunable Q-switched fiber laser based on saturable edge-state absorption in few-layer molybdenum disulfide (MoS2)," *Opt. Exp.*, vol. 22, pp. 31113–31122, Feb. 15, 2014.
[35] B. Chen, X. Zhang, C. Guo, K. Wu, J. Chen, and J. Wang, "Tungsten diselenide Q-switched erbium-doped fiber laser," *Opt. Eng.*, vol. 55, pp. 081306–081306, 2016.
[36] K. Wu, X. Zhang, J. Wang, X. Li, and J. Chen, "WS2 as a saturable absorber for ultrafast photonic applications of mode-locked and Q-switched lasers," *Opt. Exp.*, vol. 23, pp. 11453–11461, May 4, 2015.
[37] B. Chen, X. Zhang, K. Wu, H. Wang, J. Wang, and J. Chen, "Q-switched fiber laser based on transition metal dichalcogenides MoS2, MoSe2, WS2, and WSe2," *Opt. Exp.*, vol. 23, pp. 26723–26737, Oct. 5, 2015.
[38] N. Nishizawa *et al.*, "All-polarization-maintaining Er-doped ultrashort-pulse fiber laser using carbon nanotube saturable absorber," *Opt. Exp.*, vol. 16, pp. 9429–9435, Jun. 23, 2008.
[39] G. Sobon, J. Sotor, and K. M. Abramski, "All-polarization maintaining femtosecond Er-doped fiber laser mode-locked by graphene saturable absorber," *Laser Phys. Lett.*, vol. 9, p. 581, 2012.
[40] G.-Z. Zhao, X.-S. Xiao, F. Meng, J.-W. Mei, and C.-X. Yang, "An all-polarization-maintaining repetition-tunable erbium-doped passively mode-locked fiber laser," *Chin. Phys. B*, vol. 22, 2013, Art. no. 104205.
[41] P. Tonndorf *et al.*, "Photoluminescence emission and Raman response of monolayer MoS2, MoSe2, and WSe2," *Opt. Exp.*, vol. 21, pp. 4908–4916, Feb. 2013.
[42] Y. Chen *et al.*, "Mechanically exfoliated black phosphorus as a new saturable absorber for both Q-switching and mode-locking laser operation," *Opt. Exp.*, vol. 23, pp. 12823–12833, May 18, 2015.